PHYSICAL REVIEW B VOLUME 56, NUMBER 20 15 NOVEMBER 1997-II

# Silicon network relaxation in amorphous hydrogenated silicon

Z. Remeš and M. Vaněček
*Institute of Physics, Academy of Sciences of the Czech Republic, Cukrovarnická 10, CZ-162 53 Prague 6, Czech Republic*

A. H. Mahan and R. S. Crandall
*National Renewable Energy Laboratory, 1617 Cole Boulevard, Golden, Colorado 80401*

(Received 22 May 1997)

We have investigated nanovoid-free, low-defect-density, amorphous hydrogenated silicon, *a*-Si:H, with variable hydrogen content. We have observed reconstruction of all silicon-silicon bonds at temperatures as low as 430 °C, well below the crystallization temperature. This bond reconstruction leads to a decrease in thin-film thickness and an increase in material density, about 3% for the material with 9 at. % of hydrogen, during slow hydrogen outdiffusion. These results suggest that a long-range structural rearrangement of the silicon network can occur simultaneously with hydrogen motion and this has important consequences for all metastability models in amorphous hydrogenated silicon.
[S0163-1829(97)50944-1]

Hydrogenated amorphous silicon, *a*-Si:H, is not in complete thermodynamic equilibrium, as is crystalline silicon. Nevertheless many of its properties can be described by equilibrium thermodynamic models,[1,2] the most widespread being the hydrogen glass model (HGM).[3,4] This model treats amorphous hydrogenated silicon as an alloy (typically $Si_{0,9}H_{0,1}$) where hydrogen plays a very important role. This alloy consists of a fairly rigid silicon bonding matrix and a glasslike hydrogen submatrix. Above the so-called ''equilibration temperature'' (about 220 °C in undoped material[4,5]) hydrogen can move, resulting in an equilibrium between weak Si-Si bonds and Si dangling bonds.

The midgap defects (threefold-coordination defects, dangling bonds) in undoped material, which we will discuss here, are determined by equilibrium chemical reactions and their density can be calculated from thermodynamic arguments. According to the HGM, in the process of equilibration of a typical material with about $4.5\times10^{22}$ cm$^{-3}$ Si atoms and $0.5\times10^{22}$ cm$^{-3}$ H atoms, about $10^{16}$ cm$^{-3}$ Si dangling bonds are created at temperatures above the equilibration temperature from a pool of the order of $10^{19}$ cm$^{-3}$ silicon weak bonds. More than 99.9% of the silicon atoms do not move during the equilibration process.[4]

In this paper we pose the fundamental question: is the matrix of Si atoms really rigid at the temperatures well below the amorphous-crystalline transition or is there a true equilibration of the whole silicon-hydrogen network? What happens when the hydrogen is very slowly driven out? Will a significant lattice reconstruction occur; is there a measurable shrinkage of the thin film? HGM gives us no prediction in this respect. The answer to this question is important for an understanding of the crucial problem in the field of amorphous hydrogenated silicon, which is the metastability of this material (creation of additional, equilibrium density of metastable Si dangling bonds by light, which decreases the efficiency of solar cells).[4,6]

We try to answer the above question by carefully measuring the change in the film volume as hydrogen moves and slowly evolves from the material, at temperatures well below the amorphous-crystalline transition. Essentially we find that the volume shrinks as the hydrogen leaves the sample resulting in complete reconstruction, and the material density increases.

To measure the film thickness and density we use optical transmission measurements in the nonabsorbing spectral region. We precisely evaluate the interference fringes[7–9] and thereby determine the thickness and mass density of amorphous silicon thin films as a function of hydrogen content. This study is in two parts. The first part is to measure the film density in samples with differing hydrogen contents. The second part is to measure the density in films selected from the first set after hydrogen evolution.

The films in this study were of high enough electronic quality that their dangling bond density ($N_d$) was below $1\times10^{16}$ cm$^{-3}$. We concentrate on material grown by hot-wire chemical-vapor deposition (HWCVD) with H content ($c_H$) between 0.3 and 20.5 at. % (see Ref. 10). This technique can produce device-quality material with a low hydrogen content. The material also shows reduced metastability.[11,12] NMR studies show a different H microstructure of this material, compared to *material produced by the conventional* plasma-enhanced chemical-vapor deposition (PECVD).[13] The nanovoid fraction ($v_f$) in all HWCVD samples with $c_H<4$ at. % is less than 0.01% (the detection limit of small-angle x-ray scattering, SAXS).[14] Material with higher H concentration contains increasing nanovoid fractions. One PECVD sample with $v_f<0.01\%$ and $N_d\cong1\times10^{15}$ cm$^{-3}$ was measured as a control. This is quite different from previous studies where a material with substantial void fraction was examined.[15]

Approximating the imaginary part of complex dielectric constant by a $\delta$ function resonance absorption at an energy $E_R$ (Penn gap), the index of refraction as a function of photon energy can be described by two parameters [Penn gap and plasma energy ($E_P$)].[16] We made the first approximation of these two parameters from the reflectance measurement in a strongly absorbing region where no interferences are present. If $E_P$, $E_R$, and $d$ are approximately known, the full

 

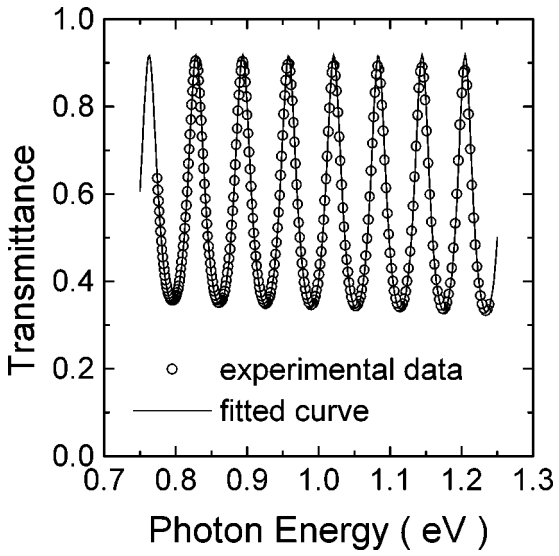


FIG. 1. Transmittance of $a$-Si:H sample, in a transparent region. The sample is HWCVD with H content of 1.6 at. %, 2.4 $\mu$m thick, deposited on Corning glass No. 7059 substrate. Experimental data points and fitted curve are shown.

spectral transmittance curve in the nonabsorbing region was simulated according to Refs. 8 and 9. A better estimate of parameters, error estimate on the parameters, and a statistical measure of goodness of fit then represent a process of optimization in many dimensions and it yields the values of thickness ($d$) and index of refraction [$n(E)$] as a function of photon energy ($E$) with a high enough precision to investigate thickness and index of refraction changes following hydrogen evolution.

The classical approach, based on the Clausius-Mossoti equation, is used to relate the index of refraction ($n_\infty$) in the long-wavelength limit with a number of Si-Si and Si-H oscillators with densities, respectively, $N_{Si\text{-}Si}$ and $N_{Si\text{-}H}$ and bond polarizabilities $\alpha_{Si\text{-}Si}$ and $\alpha_{Si\text{-}H}$ (see Ref. 17). The bond polarizability of the Si-Si bond is determined from the measured refractive index of $a$-Si:H with a negligible hydrogen content and its mass density $\rho$=2.287 g cm$^{-3}$ (see Ref. 18). The bond polarizability of the Si-H bond is taken from polarizability of the $SiH_4$ molecule.[17] Hence, knowing the concentration of bonded hydrogen from IR absorption measurements and dominant monohydride bonding (for $c_H$<12%) Ref. 22, it is possible to determine the mass density ($\rho$) from the measured index of refraction. Full technical details are given elsewhere.[19]

A computer-controlled single-beam spectrometer was used for high-precision transmission measurements in the 400–2000 nm spectral region. A stabilized tungsten-halogen lamp was used as the light source; Si and InGaAs photovoltaic and PbS photoconductive detectors were used in different spectral regions. Monochromatic light illuminated the sample through a mask with a 0.5-mm-diameter hole to suppress the influence of thickness variation of the $a$-Si:H layer. The optimum film thickness was between 0.5 and 3 $\mu$m because of the finite monochromator spectra resolution and necessity of a sufficient number of interferences. Typical experimental data together with fitted curve are given in Fig. 1.

At first we investigated a series of HWCVD samples prepared with a different hydrogen content $c_H$.[10,11] Results are given in Table I and displayed in Fig. 2. It can be seen that the density of $a$-Si:H decreases with an increasing H content. For a comparison, a conventional PECVD sample is also shown. Error bars of the mass densities have been estimated from errors of fitted indexes of refraction ($n_\infty$), which were typically around 0.005.

TABLE I. Hydrogen content $c_H$, index of refraction $n_\infty$, in the long-wavelength limit and mass density $\rho$ for series of HWCVD samples and the reference PECVD sample (GD).

| Sample | $c_H$ (%) | $n_\infty$ | $\rho$ (g cm$^{-3}$) |
|---|---|---|---|
| HW26 | 0.3 | 3.667 | 2.286 |
| HW59 | 1.6 | 3.625 | 2.271 |
| HW91 | 2.2 | 3.639 | 2.274 |
| HWth81 | 5.8 | 3.591 | 2.252 |
| GD232 | 9.0 | 3.520 | 2.225 |
| HWth62 | 11.0 | 3.501 | 2.214 |
| HW129 | 12.6 | 3.494 | 2.207 |
| HW70 | 17.0 | 3.438 | 2.178 |
| HW71 | 20.5 | 3.252 | 2.108 |

Our results presented in Table I and in Fig. 2 show that in the material with a negligible void fraction, as it is for ''device quality'' HWCVD material with hydrogen content below approximately 10 at. % and for conventional PECVD $a$-$Si_{0.91}H_{0.09}$ (see Ref. 14), the density deficiency (compared to the crystalline silicon density $\rho$=2.33 g cm$^{-3}$) comes not only from a difference between the unhydrogenated amorphous Si (prepared by ion implantation[18]) and the crystalline state, but also from ''substitution'' of Si atoms by H atoms. Lattice relaxation is not included. To describe this behavior two simple models are presented in Fig. 2. In the monovacancy model four hydrogen atoms replace one silicon atom, in the divacancy model six hydrogen atoms replace two sili-

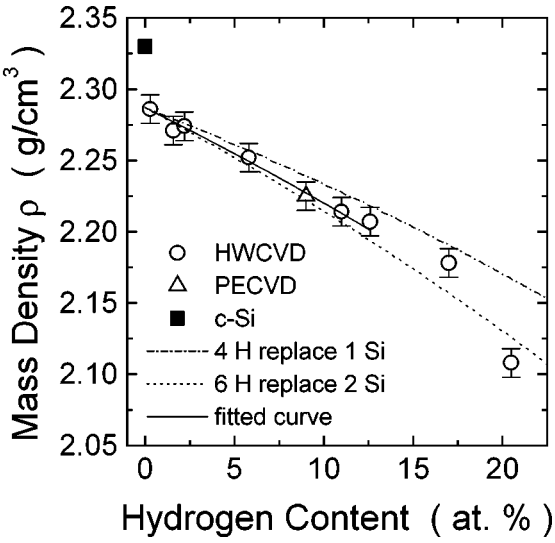


FIG. 2. Measured mass density $\rho$ of a series of HWCVD samples with a different hydrogen content $c_H$, error bars are shown too. The conventional PECVD sample is also shown for comparison. Samples are summarized in Table I. Two theoretical dependencies are simulated. Full curve is the best mix of them fitting measured densities for $c_H$<11%.

TABLE II. Hydrogen content $c_H$, thickness $d$, index of refraction $n_\infty$, and mass density $\rho$, before and after ( . . . → . . . ) annealing. Error bars of $n_\infty$ were 0.005, error bars of $d$ were 5 nm.

| | Sample | $c_H$ (%) | $d$ (nm) | $n_\infty$ | $\rho$ (g cm$^{-3}$) |
|---|---|---|---|---|---|
| Anneal at 500 °C | GD232a | 9→0 | 1902→1827 | 3.528→3.682 | 2.226→2.290 |
| 24 h | HW59 | 1.6→0 | 2418→2393 | 3.625→3.702 | 2.271→2.295 |
| Anneal at 460 °C | GD232b | 9→≈0 | 1971→1869 | 3.512→3.675 | 2.222→2.288 |
| 100 h | HWth81a | 5.8→≈0 | 828→808 | 3.530→3.645 | 2.235→2.279 |
| Anneal at 430 °C | HWth81b | 5.8→≈1 | 737→728 | 3.582→3.656 | 2.250→2.283 |
| 100 h | | | | | |

con atoms. If we fit the data for $c_H<11$ at. % then the best mix of these two dependencies gives $70\pm10$ % of divacancies and 30% of monovacancies presented in the void-free material. A much lower density is typically observed for material with a hydrogen content higher than 11 at. %; nanovoids are the reason for this density deficit.[15]

To examine changes in the material density and layer thickness with a gradual hydrogen evolution, the samples were cut into several pieces and these were very slowly annealed above their deposition temperature in a flow of ultrapure molecular hydrogen. The heating rate was 1 °C/min. and the cooling rate was 0.5 °C/min. The annealing time was 24–100 h, depending on the annealing temperature and sample thickness. Thinner samples (less than 1 $\mu$m) and longer times were used for annealing at 460 and 430 °C. Before and after annealing all surfaces appeared mirrorlike. In contrast to Ref. 20 no cracks were observed under the optical microscope. Three samples with hydrogen contents of 9, 5.8, and 1.6 at. % were slowly annealed at 500, 460, and 430 °C to evolve hydrogen. The sample with 9 at. % H was standard PECVD material. Deposition temperature was 250 °C. The medium and low hydrogen content material (5.8 and 1.6 at. %) were deposited by HWCVD at substrates 320 and 370 °C, respectively.

Subgap optical-absorption measurement with the help of the constant photocurrent method and calibrated by electron spin resonance (ESR) was used to monitor the defect density.[21] It was observed to saturate at $5\times10^{18}-1\times10^{19}$ cm$^{-3}$ for samples with more than 99% of H evolved,[21] in accord with another study where ESR was used to measure defect density.[20] This means that 99.9% of the Si bonds reconstruct during H evolution. Otherwise many more defects would be produced. Annealing times for a given temperature and sample thickness are consistent with our H evolution data.[22] Great care was taken to ensure transmission measurement of samples before and after annealing at the same spot. Typically the thickness and index of refraction were averaged from several measurements with reproducibility better than 0.5%.

The results are summarized in Table II. Here the value of a long-wavelength limit of the index of refraction $n_\infty$, mass density $\rho$, and thickness $d$ is given before and after anneal.

Figure 2 shows that the $a$-Si:H density decreases with an increasing hydrogen content $c_H$. Our new observation (look at Table II) is that this effect is reversible: slowly evolving hydrogen increases the mass density back to the original value corresponding to the unhydrogenated void-free material. Density and thickness of the layer with just partly evolved hydrogen is in between its initial and final value.

Our data presented in Table II conclusively show that the void-free $a$-Si:H layer shrinks during slow hydrogen evolution, hence, all atoms have to move and reconfigure their relative position. This new observation has a strong consequence for metastability models in $a$-Si:H. It means that up to the present time rather speculative metastability model considering long-range structural rearrangements of the amorphous network, involving thousands of atoms for each defect created,[23] is quite plausible. In contrast to this, the widespread hydrogen glass model assumes that just the weakly bonded Si atoms reconfigure only on a local scale due to a hydrogen diffusion.

In conclusion, we have investigated void-free, low-defect, amorphous hydrogenated silicon prepared by different deposition techniques. The mass density of this material decreases with an increasing hydrogen content. Slowly evolving hydrogen from the material increases the mass density to the original value corresponding to the unhydrogenated void-free material. We have shown that a complete reconstruction of silicon bonds proceeds in this material at temperatures as low as 430 °C, well below the crystallization temperature. This bond reconstruction leads to a decrease in layer thickness and increase of material density, about 3% for the material with 9 at. % of hydrogen, after H evolution. Metastability in amorphous hydrogenated silicon can involve rearrangement of Si lattice on a large scale.

The authors acknowledge support of the US-Czech Science and Technology Program, Grant No. 93074.

[1] R. A. Street and K. Winer, Phys. Rev. B **40**, 6236 (1989).

[2] Z. E. Smith and S. Wagner, in *Amorphous Silicon and Related Materials*, edited by H. Fritzsche (World Scientific, Singapore, 1989), p. 409.

[3] R. A. Street, J. Kakalios, and T. M. Hayes, Phys. Rev. B **34**, 3030 (1986).

[4] R. A. Street, *Hydrogenated Amorphous Silicon* (Cambridge University Press, Cambridge, UK, 1991).

[5] M. Vaněček and A. H. Mahan, J. Non-Cryst. Solids **190**, 163 (1995).

[6] D. L. Staebler and C. R. Wronski, Appl. Phys. Lett. **31**, 292 (1977).

[7] L. Ward, *The Optical Constants of Bulk Materials and Films*, 2nd ed. (Institute of Physics, Bristol, 1994).
[8] R. Swanepool, J. Phys. E **16**, 1214 (1983).
[9] R. Swanepool, J. Phys. E **17**, 896 (1984).
[10] A. H. Mahan, J. Carapella, B. P. Nelson, R. S. Crandall, and I. Balberg, J. Appl. Phys. **69**, 6728 (1991).
[11] A. H. Mahan and M. Vaněček, in *Amorphous Silicon Materials and Solar Cells*, Proceedings of the International Meeting on Stability of Amorphous Silicon Materials, edited by B. L. Stafford, AIP Conf. Proc. No. 234 (AIP, New York, 1991), p. 195.
[12] D. Kwon, J. D. Cohen, B. P. Nelson, and E. Iwaniczko, in *Amorphous Silicon Technology–1995*, edited by M. Hack, E. A. Schiff, M. Powell, A. Matsuda, and A. Madan, MRS Symposia Proceedings No. 377 (Materials Research Society, Pittsburgh, PA, 1995), p. 301.
[13] Y. Wu, J. T. Stephens, D. X. Han, J. M. Rutland, R. S. Crandall, and A. H. Mahan, Phys. Rev. Lett. **77**, 2049 (1996).
[14] D. L. Williamson, in *Amorphous Silicon Technology–1995* (Ref. 12), p. 251.
[15] C. Manfredotti, F. Fizzotti, M. Boero, P. Pastorino, P. Polesello, and E. Vittone, Phys. Rev. B **50**, 18 046 (1994).
[16] G. D. Cody, in *Hydrogenated Amorphous Silicon, Semiconductors and Semimetals*, edited by J. Pankove (Academic Press, New York, 1984), Vol. 21, Pt. C, p. 11.
[17] J. C. van den Heuvel, M. J. Geerts, and J. W. Metselaar, Sol. Energy Mater. **22**, 185 (1991).
[18] J. S. Custer, M. O. Thompson, D. C. Jacobson, J. M. Poate, S. Roorda, W. C. Sinke, and F. Spaepen, Appl. Phys. Lett. **64**, 437 (1994).
[19] Z. Remeš, M. Vaněček, U. Kroll, A. H. Mahan, and R. S. Crandall, J. Non-Cryst. Solids (to be published).
[20] J. H. Zhou, M. Kumeda, and T. Shimizu, J. Non-Cryst. Solids **195**, 76 (1996).
[21] M. Vaněček, J. Fric, A. Poruba, A. H. Mahan, and R. S. Crandall, J. Non-Cryst. Solids **198-200**, 478 (1996).
[22] A. H. Mahan, E. J. Johnson, R. S. Crandall, and H. M. Branz, in *Amorphous Silicon Technology–1995* (Ref. 12), p. 413.
[23] D. P. Masson, A. Ouhlal, and A. Yelon, J. Non-Cryst. Solids **190**, 151 (1995).